Lithium in Ammonia

DOI: 10.1002/anie.200604431

Creating Interfaces by Stretching the Solvent Is Key to Metallic Ammonia Solutions**

Amalendu Chandra* and Dominik Marx*

Although the phenomenon of electron solvation has been known for at least one and a half centuries,[1,2] explanations of the detailed behavior of solvated electrons in molecular liquids, in particular in metal/ammonia solutions,[1–3] have remained controversial. At low concentrations, metal/ammonia solutions behave like electrolytes whereas they undergo a transition to a metallic liquid—heralded by changing their color from blue to bronze—on increasing the metal content.[2,3] Also, adding metal lowers the density of the solution drastically compared to the neat liquid. This is thought to lead to the formation of voids hosting the unbound electrons,[4,5] which percolate at sufficiently high metal content.[6,7] Distinct from this viewpoint is a more chemical perspective[8,9] whereby the solvated electron in ammonia is believed to be some sort of open-shell molecular species and, in the limiting case, even an anionic radical as such. However, with increasing concentration close to saturation the influence of the metal ion cores, particularly their solvation and ion-pair formation, can no longer be neglected. Indeed, recent diffraction data of Li/NH_3 solutions up to 21 mol% metal (21 MPM) clearly demonstrate that they are highly structured over both the short and intermediate length scales.[10] In particular, the studies suggest that these solutions can be constructed from two major structural units: tightly bound $[Li(NH_3)_4]^+$ tetrahedra and empty voids.[10] In addition, inelastic X-ray scattering close to the saturation limit uncovered not only plasmon resonances and strong deviations from the Jellium model of simple metals, but also excitations that are associated with vibrations of these quasimolecular complexes.[11] Finally, the protonic self-diffusion coefficient is nonmonotonic in the liquid state; it first increases with metal concentration before decreasing again on reaching saturation, an observation that is explained in terms of competing influences of electron and ion solvation.[12] Together these novel findings raise the question of how the intricate real-space structure and the delocalized electronic structure are interrelated in the metallic liquid.

Unfortunately, known density functionals do not provide the correct structure and energetics of the ammonia–ammonia interactions in that they predict an essentially linear hydrogen bond for the dimer, similar to classical force field models.[13] To cure this deficiency in the description of the solvent the HCTH/407+ functional[13] has been designed for the simulation of ammonia systems. By using HCTH/407+, a 21-MPM lithium/ammonia solution at 230 K was simulated in terms of 6 Li and 23 NH_3 in a periodic box of 11.314 Å by diagonalizing the finite-temperature free-energy functional[14,15] iteratively as implemented in CPMD[15,16] to account for metallicity in terms of partially occupied Kohn–Sham orbitals. The orbitals were expanded in plane waves at the Γ point up to 50 Ry, H and N were represented as usual by one and five valence-electron Goedecker-type pseudopotentials, whereas an all-electron Goedecker-type treatment turned out to be necessary for Li. The system was equilibrated for about 6 ps at 230 K in the NVT ensemble followed by a 10-ps NVE run for analysis with a time step of 20 a.u. and the mass of D for the hydrogen atoms in order to minimize quantum effects. In addition, reference calculations on pure ammonia at 230 K and different densities were carried out.[13]

Both the cavity and spatial distribution functions (CDFs and SDFs) of the 21-MPM solution closely match the experimental data[10] according to Figure 1 a and Figure 2 a,b. Also the nontrivial concentration-dependent self-diffusion properties revealed by recent experiments[12] are qualitatively reproduced. In particular, the diffusion coefficient of deuterated ammonia is found to increase by a factor of about 1.4 (from ca. $1.7\times10^{-5}\,cm^2s^{-1}$ for pure ammonia to ca. $2.4\times10^{-5}\,cm^2s^{-1}$ for the 21-MPM solution), which compares to an experimental factor of 1.3.[12] Finally, the partial radial distribution functions (RDFs) are consistent with neutron diffraction data;[10] in particular, the weak hydrogen bonding of the pure liquid is completely destroyed in the 21-MPM solution (data not shown).

In the framework of ab initio simulations such an agreement with detailed experimental data testifies to a faithful description of the underlying electronic structure. This provides confidence that the simulation data can be used to supplement the diffraction data by "adding-in the electrons", thereby establishing, most directly, the missing link between real-space structure and electronic structure without the need to searching for "the dog that did not bark" (as cited from Sherlock Holmes in reference [10b]). The key here is the

---

[*] Prof. Dr. A. Chandra
Department of Chemistry
Indian Institute of Technology
Kanpur 208016 (India)
Fax: (+91) 512-259-7436
E-mail: amalen@iitk.ac.in
Homepage: http://www.iitk.ac.in/chm/CHM/ac.htm

Prof. Dr. A. Chandra, Prof. Dr. D. Marx
Lehrstuhl für Theoretische Chemie
Ruhr-Universität Bochum
44780 Bochum (Germany)
E-mail: dominik.marx@theochem.rub.de
Homepage: http://www.theochem.rub.de

[**] We are grateful to A. Alavi, H. Langer, and S. Yashonath for discussions. Partial support was provided to A.C. by a Humboldt Fellowship and to D.M. by DFG and FCI. The simulations were carried out on hardware granted to A.C. by AvH and Department of Science and Technology (Government of India), and at BOVILAB@RUB.

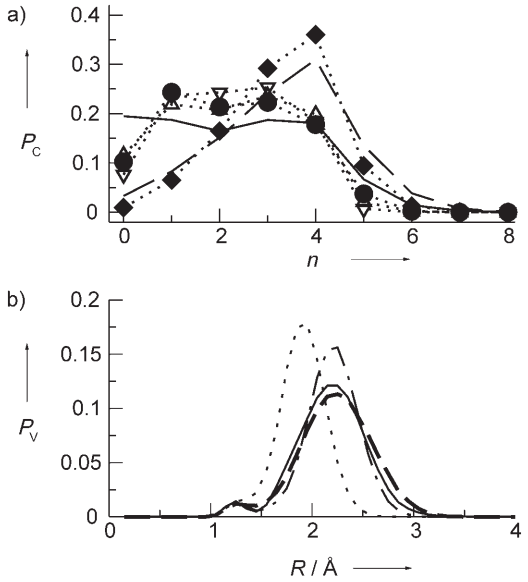

Figure 1. a) Cavity distribution functions (CDFs) for 21-MPM solution (filled circles), pure ammonia at equilibrium density (filled diamonds), pure ammonia expanded to the density of the 21-MPM solution (upward triangles), and pure ammonia at equilibrium density scaled to the 21-MPM density (downward triangles); dotted lines are guides to the eye, and experimental data of the 21-MPM solution and pure ammonia are shown by solid and dashed lines, respectively. These functions[10b] measure the probability to find n atoms of any kind in a sphere of 2-Å radius centered at the vertices of a real-space grid of 0.2-Å spacing, and empty cavities are defined by $n = 0$; changing sphere radius or grid spacing in reasonable bounds does not alter the conclusions. b) Void distribution functions (VDFs) for 21-MPM solution (solid), pure ammonia at equilibrium density (dotted), pure ammonia at expanded density (dashed), and pure ammonia at scaled density (dash-dotted). These functions measure the probability to find empty spherical voids of radius R (within $R \pm 0.05$ Å), taking into account the ion cores of N, Li, and H as point particles.

decomposition of the electronic structure into those orbitals that can be uniquely assigned to the ion cores, and those that cannot. By using maximally localized Wannier functions,[17] subsets of eight electrons can be clearly assigned to each ammonia molecule (to form three covalent N–H bonds and one lone pair per NH_3 molecule, data not shown) and two to each Li^{3+} core (yielding the tight $1s^2$ inner shell within the all-electron treatment and thus the monovalent Li^+ cations, data not shown). The remaining six electrons are essentially spread over seven fractionally occupied orbitals (with typical occupation numbers of about 2.0, 1.5, 0.9, …, 0.1), have a much larger width, and cannot be attached to any particular ionic core, so that they are considered to be "unbound". Analysis of the radial structure of the corresponding Wannier function centers (WFCs) relative to the atomic cores by using the RDFs in Figure 3 first of all shows that these unbound electrons clearly avoid the N cores and even more so the Li ions.

Nevertheless, clear radial structure is visible in both cases, which can be orientationally unfolded by using the SDFs in Figure 2a,b. With respect to the N cores, the RDF peak close to 2.75 Å can be assigned in the SDFs to unbound electrons (blue) that accumulate preferentially close to the H atoms but outside the NH_3 molecules; this is reminiscent of the conduction band in the crystal.[7] Since the Li cores (green) are well localized with respect to the dipole axes of the NH_3 molecules in the $[Li(NH_3)_4]^+$ tetrahedra, the very same unbound electrons are also responsible for the pronounced peak of the Li-WFC RDF at about 3.7 Å in Figure 3a; this arrangement also leads to maxima in the H-WFC RDFs around 1.5 and 3.1 Å. Most importantly, the spatial distribution of the empty cavities (red in Figure 2) is seen to preferentially occupy the upper hemisphere around the NH_3 molecules, except for those regions in space, close to the H atoms, where the unbound electrons prefer to reside; in a geometrical sense, the NH_3 pyramids straddle the empty cavities. Thus, the regions of preferential localization for empty cavities and unbound electrons are mutually exclusive

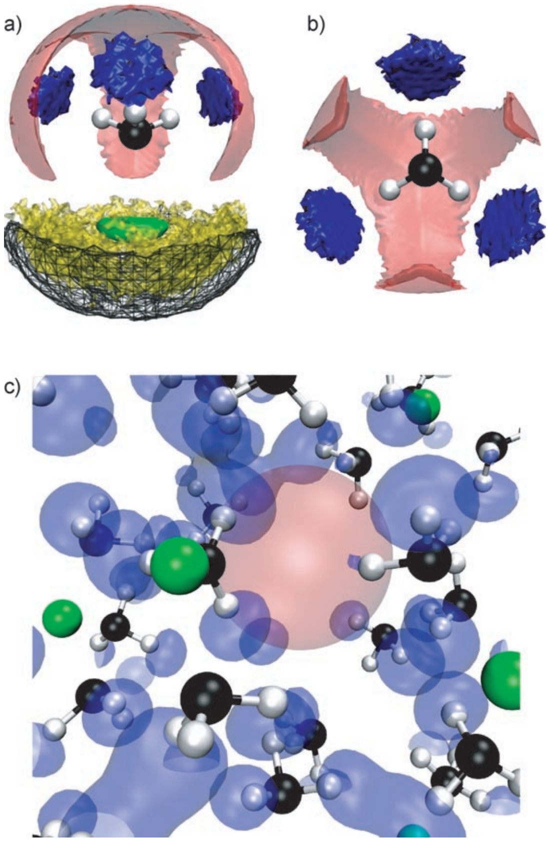

Figure 2. a, b) Spatial distribution functions (SDFs) with respect to the NH_3 molecules showing the relative density distribution of N cores (black grid, with a distance cutoff of 4.0 Å relative to the N core), Li cores (green, with a cutoff of 3.0 Å relative to N), Wannier function centers of the unbound electrons (blue and yellow, with cutoff ranges of 2.5–3.5 and 1.75–2.25 Å relative to N and Li, respectively, and a much smaller isosurface value for the latter), and empty cavity centers (red, with a cutoff of 4.5 Å relative to N). The N core of NH_3 defines the origin of the coordinate system, the z axis is defined by the geometric dipole moment, the orientation is fixed by rotating one N–H bond in the xz plane, and the SDFs are averaged with respect to the three possible orientations. Different perspectives are presented in a) and b), where in the latter only the SDFs close to the H cores are depicted for clarity. c) Representative configuration snapshot (partial view) displaying an empty cavity of 2.0-Å radius (red) and the corresponding electronic density of the unbound electrons (blue).

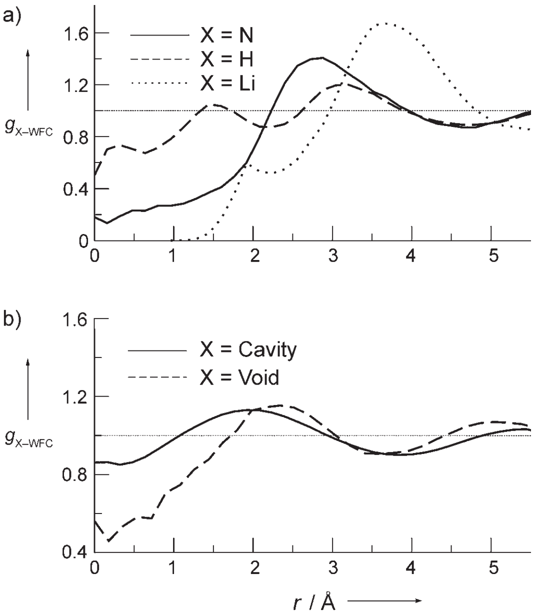

Figure 3. Radial distribution functions (RDFs) of the 21-MPM solution involving the Wannier function centers (WFCs) of the unbound electrons. a) N WFC (solid), H WFC (dashed), and Li WFC (dotted). b) Empty cavity-center WFC (solid) and void WFC (dashed). Dotted horizontal lines mark the $r \rightarrow \infty$ uniform limit.

and even complementary. The black net showing the density of N atoms corresponds to the average locations of the other three N atoms of the same $[Li(NH_3)_4]^+$ tetrahedra to which the N atom at the origin belongs. The unbound electrons (yellow) in the lower part of Figure 2a correspond to those WFCs which give rise to the small feature close to 2 Å in the Li-WFC RDF (see Figure 3a).

The above picture is also consistent with the cavity-center-WFC RDF in Figure 3b, which clearly features no increased density of unbound electrons close to the empty cavity centers as $r \rightarrow 0$. Rather, a broad peak revealing the preferential presence of unbound electrons is found at about 2.0 Å, that is, far away from the centers of the empty cavities, a trend which is more pronounced for the void-WFC RDF (see below). Evaluating a partial SDF taking only these unbound electrons into account (data not shown) demonstrates that they are the unbound electrons (blue) in Figure 2a,b which are close to the H atoms. Furthermore, they are also responsible for the H-WFC radial structure in Figure 3a, which displays a small but significant accumulation of unbound electrons at about 1.5 Å from H atoms. In summary, the enhanced probabilities that appear as peaks at about 1.5 and 3.1 Å in the H-WFC RDF and at about 2.75, 3.7, and 2.0 Å in N-, Li-, and cavity-WFC RDFs, respectively, can all be assigned to those unbound electrons which reside near the H atoms right at the cavity/solvent interfaces. The typical snapshot in Figure 2c depicts this arrangement in real space: the Li cores (green) are far from the cavities (red), and the latter are not preferentially occupied by the unbound electrons (blue). Rather, the unbound electrons accumulate preferentially at the interfacial regions.

The metallic solution at 21 MPM is characterized by the presence of a significant number of empty cavities according to the CDF in Figure 1a, whereas the propensity of the pure liquid to form empty cavities of this size is small. Are these empty cavities induced by the unbound electrons in the concentrated solution? To address this, pure ammonia was expanded to the density of the 21-MPM solution. Astonishingly, the CDF of this stretched ammonia quantitatively reproduces that of the metallic solution (see Figure 1a). Even the uniform scaling of all intermolecular distances sampled from the trajectory of the pure liquid at its equilibrium density to the much lower 21-MPM density yields a similar match with the true 21-MPM data. Complementing this cavity analysis, an alternative to investigate void regions is to obtain Delaunay tessellations in real space from Voronoi constructions. As expected, the void distribution function (VDF) of the concentrated solution is centered at significantly larger sphere radii compared to the pure liquid, as depicted in Figure 1b. Moreover, not only the CDF but also the VDF of the metallic liquid can be mimicked by either expanding or just scaling the pure ammonia system; the average sphere radii are 2.2 Å for the metallic, stretched, and scaled systems, as compared to 1.9 Å for pure ammonia at its equilibrium density. Thus, increasing the interfacial regions that are already available in the liquid, though to a much lesser extent, seems to be the major density effect in this expanded metal.

Certainly there is a “chicken-and-egg issue” here, but it is evident that a very similar real-space structure with regard to the voids in metallic solutions can be generated without any unbound electrons by simply stretching or scaling the pure liquid. This is in accord with the finding that the unbound electrons do not preferentially accumulate at the centers of the cavities, but rather at the interfacial regions. Qualitatively, this can be understood as an electrostatic polarization shell around the positively charged $[Li(NH_3)_4]^+$ building blocks establishing these interfacial regions. The spatial anisotropy, however, has a chemical origin: the Li^+ cores in the tetrahedra polarize via the lone pairs the NH_3 molecules in their first solvation shells and induce an attractive positive partial charge at the hydrogen atoms ($H^{\delta+}$) which are right at the cavity/solution interface.

The finding that the unbound electrons in strongly metallic ammonia solutions do not preferentially populate the void regions is in harmony with the explanation that the unbound (or anionic) electrons in insulating electrides are actually trapped at the void centers.[18] In conducting metal/ammonia solutions, on the contrary, one could say that the cavities are not only void of atoms but also have a low density of unbound electrons, which have a propensity to accumulate at the void/solvent interface. In the light of these findings, it appears that both the formation of such interfacial regions by stretching the liquid and the chemical involvement of the solvent at the interfaces are crucial to understand the metallic state. In more general terms, shifting the focus to interfacial regions might be the key to understanding electronic properties of solvated electrons in molecular systems.

Received: October 29, 2006
Revised: January 30, 2007

Keywords: ab initio calculations · ammonia · electronic structure · interfaces · lithium · molecular dynamics

---

[1] W. Weyl, *Ann. Phys. Chem.* **1864**, *121*, 601 – 612.
[2] P. P. Edwards, *Adv. Inorg. Chem. Radiochem.* **1982**, *25*, 135 – 185.
[3] J. C. Thompson, *Electrons in Liquid Ammonia*, Clarendon, Oxford, **1976**; N. F. Mott, *Metal-Insulator Transitions*, Taylor & Francis, London, **1990**.
[4] R. A. Ogg, Jr., *Phys. Rev.* **1946**, *69*, 668 – 669.
[5] J. Jortner, *J. Chem. Phys.* **1959**, *30*, 839 – 846.
[6] M. Sprik, R. W. Impey, M. L. Klein, *Phys. Rev. Lett.* **1986**, *56*, 2326 – 2329; Z. Deng, G. J. Martyna, M. L. Klein, *Phys. Rev. Lett.* **1992**, *68*, 2496 – 2499; Z. Deng, G. J. Martyna, M. L. Klein, *Phys. Rev. Lett.* **1993**, *71*, 267 – 270; Z. Deng, M. L. Klein, G. J. Martyna, *J. Chem. Soc. Faraday Trans.* **1994**, *90*, 2009 – 2013.
[7] J. Kohanoff, F. Buda, M. Parrinello, M. L. Klein, *Phys. Rev. Lett.* **1994**, *73*, 3133 – 3136; see also Comment: T. A. Kaplan, J. F. Harrison, J. L. Dye, R. Rencsok, *Phys. Rev. Lett.* **1995**, *75*, 978 – 978.
[8] T. R. Tuttle, Jr., S. Golden, *J. Phys. Chem.* **1991**, *95*, 5725 – 5736.
[9] I. A. Shkrob, *J. Phys. Chem. A* **2006**, *110*, 3967 – 3976.
[10] a) S. Hayama, N. T. Skipper, J. C. Wasse, H. Thompson, *J. Chem. Phys.* **2002**, *116*, 2991 – 2996; b) H. Thompson, J. C. Wasse, N. T. Skipper, S. Hayama, D. T. Bowron, A. K. Soper, *J. Am. Chem. Soc.* **2003**, *125*, 2572 – 2581; c) H. Thompson, J. C. Wasse, N. T. Skipper, C. A. Howard, D. T. Bowron, A. K. Soper, *J. Phys. Condens. Matter* **2004**, *16*, 5639 – 5652.
[11] C. A. Burns, P. Giura, A. Said, A. Shukla, G. Vankó, M. Tuel-Benckendorf, E. D. Isaacs, P. M. Platzman, *Phys. Rev. Lett.* **2002**, *89*, 236404; C. A. Burns et al., *J. Chem. Phys.* **2006**, *124*, 024720.
[12] H. Thompson, N. T. Skipper, J. C. Wasse, W. S. Howells, M. Hamilton, F. Fernandez-Alonso, *J. Chem. Phys.* **2006**, *124*, 024501.
[13] A. D. Boese, A. Chandra, J. M. L. Martin, D. Marx, *J. Chem. Phys.* **2003**, *119*, 5965 – 5980.
[14] A. Alavi, J. Kohanoff, M. Parrinello, D. Frenkel, *Phys. Rev. Lett.* **1994**, *73*, 2599 – 2602.
[15] D. Marx, J. Hutter in *Modern Methods and Algorithms of Quantum Chemistry* (Ed.: J. Grotendorst), NIC, FZ Jülich, **2000**, pp. 301 – 449; see http://www.theochem.rub.de/go/cprev.html.
[16] J. Hutter et al., CPMD; see http://www.cpmd.org.
[17] N. Marzari, D. Vanderbilt, *Phys. Rev. B* **1997**, *56*, 12847 – 12865.
[18] J. L. Dye, *Science* **1990**, *247*, 663 – 668; J. L. Dye, *Science* **2003**, *301*, 607 – 608.